Chinese Journal of
POLYMER SCIENCE

ARTICLE

https://doi.org/10.1007/s10118-018-2067-1
Chinese J. Polym. Sci. 2018, 36, 703–711

Perylene Bisimide In-chain Polyethylene with Unique Self-assembly Nanostructure through Acyclic Diene Metathesis (ADMET) Polymerization

Wei Song[a*], Yang You[a], Tian-Jing Li[c], Juan Li[a], and Liang Ding[a, b*]

[a] *Department of Polymer and Composite Material, School of Materials Engineering, Yancheng Institute of Technology, Yancheng 224051, China*
[b] *Roy & Diana Vagelos Laboratories, Department of Chemistry, University of Pennsylvania, Philadelphia 19104-6323, PA, USA*
[c] *School of Automotive Engineering, Yancheng Vocational Institute of Industry Technology, Yancheng 224005, China*

Electronic Supplementary Information

Abstract A novel perylene tetracarboxylic acid bisimide (PTCBI) in-chain polyethylene (PE) was first prepared *via* acyclic diene metathesis (ADMET) polymerization of PTCBI-functionalized α,ω-diene monomer. The polymers could spontaneously self-assemble into hollow cylindrical structures in which the π-π interaction between adjacent PTCBI moieties was enhanced and the electron mobility was possibly promoted. The hydrogenation of as-obtained polymer was readily accomplished, affording the desired precision PTCBI in-chain PE with a saturated backbone, which showed high glass transition temperature (T_g = 63 °C), relatively wide range of light absorption (λ = 200−575 nm), and higher LUMO level (−3.62 eV). It can therefore serve as a superior model for facile construction of functional polyolefin and soluble PTCBI polymer with ordered architecture.

Keywords Acyclic diene metathesis polymerization; Hydrogenation; Polyethylene; Perylene bisimide

Citation: Song, W.; You, Y.; Li, T. J.; Li, J.; Ding, L. Perylene Bisimide In-chain Polyethylene with Unique Self-assembly Nanostructure through Acyclic Diene Metathesis (ADMET) Polymerization. Chinese J. Polym. Sci. 2018, 36(6), 703–711.

INTRODUCTION

Perylene tetracarboxylic acid bisimide derivatives (PTCBIs) combine highly planar π-conjugated cores with electron-withdrawing tetracarboxydiimide, and substitutes on imide nitrogen can manipulate solubility, morphology, and solid-state packing without disrupting backbone electronic conduction[1]. Therefore, they are promising building block candidates not only in the field of organic electronics applications, but also for the construction of supramolecular structures since the functional groups can be flexibly introduced to either the terminal imide moiety or the bay positions of perylene core for creating multifunctional molecules[2–7].

The strong tendency of π-π stacking interaction can offer the PTCBI-containing polymers distinct aggregates and nanophases, which ultimately endow them with disparate properties, even though the polymers have the same composition. The effect of molecular stacking and ordered degree within the nanophase on the performance of PTCBI-based organic photovoltaic devices (OPVs) has been demonstrated, which played a fundamental role on the electron transport, the balance of charge carrier and non geminate recombination losses[8]. Therefore, a systematic design and study of PTCBI-containing polymers with controlled morphology are essential. The precise control can be achieved by using the acyclic diene metathesis (ADMET) polymerization as a powerful and broadly applicable method, to introduce the precise placement of functional groups either in the polymer backbone or pendant side-chains[9–13]. This periodic sequence encoded in the final polyolefin can be predetermined through a tail-made α,ω-diene monomer. The precision polymers may lead to unique morphologies that help to further elucidate the morphology of PTCBI-containing polymer systems, as well as potentially enhance their performance.

Recently, we designed and synthesized a polymer with interpenetrating network by introducing strong π-π interactions on the side-chain to promote kinetically trapped self-assembly. In order to clarify the influence of π-π interaction on the morphology and inherent crystalline behavior of the resulting polymers in detail, a PTCBI-functionalized α,ω-diene monomer was first synthesized. Then linear high molecular weight polyethylenes (PEs) with bulky PTCBI moieties (PTCBI defects) precisely placed on every 42nd methylene units along the backbone were successfully produced *via* ADMET polymerization and subsequently hydrogenated (Scheme 1). The precision PTCBI in-chain PEs showed highly ordered architecture, good

* Corresponding authors: E-mail sw121092@ycit.cn (W.S.)
E-mail dl1984911@ycit.edu.cn (L.D.)
Received September 16, 2017; Accepted October 17, 2017; Published online February 13, 2018

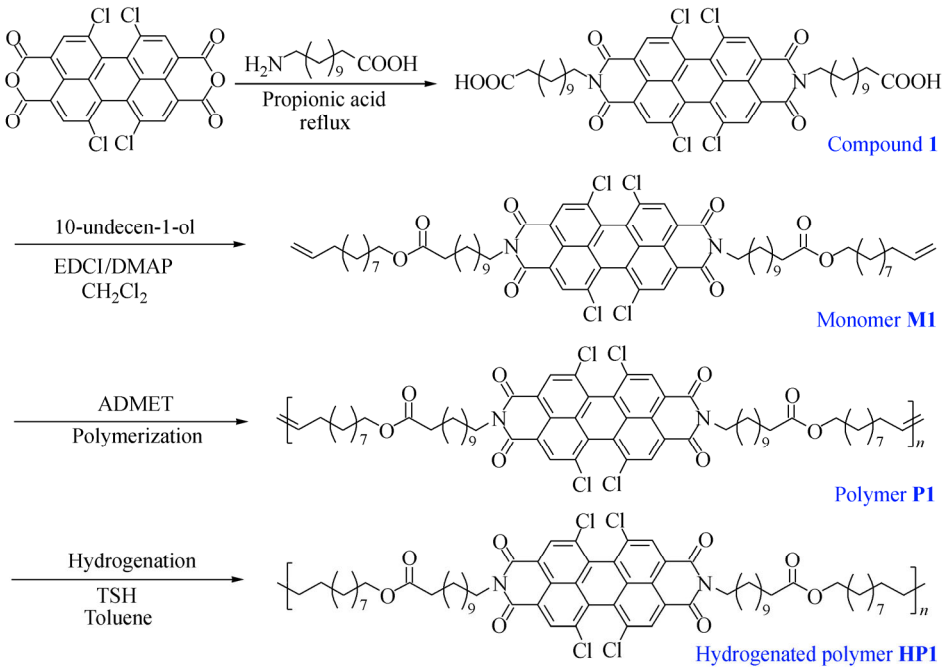

Scheme 1 Schematic representation of the synthesis of perylene bisimide in-chain polyethylene *via* ADMET polymerization

thermal stability, and optoelectronic properties. In addition, the polymers can self-assemble into a unique architecture.

EXPERIMENTAL

Materials

12-Aminododecanoic acid, 10-undecen-1-ol, and [1,3-bis(2,4,6-trimethylphenyl)-4,5-dihydroimid-azol-2-ylidene] benzylidene ruthenium dichloride (Grubbs second generation catalyst, **Ru-II**) were obtained from Aldrich. Ethyl vinyl ether (stabilized with 0.1% *N*,*N*-diethyl aniline) was purchased from Acros. 1,6,7,12-Tetrachloroperylene-3,4,9,10-tetracarboxylic dianhydride (TCPTCDA) with analytical grade was purchased from commercial source and used without further purification. *p*-Toluenesulfonohydrazide (TSH), butylated hydroxytoluene (BHT), 1-(3-dimethylaminoprop-yl)-3-ethyl-carbodiimidehydrochloride (EDCI·HCl), and 4-dimethyl-aminopyridine (DMAP) were purchased from Energy Chemical. All reactions were carried out under dry nitrogen atmosphere using standard Schlenk-line techniques. The solvents including dichloromethane (CH_2Cl_2), chloroform ($CHCl_3$), and toluene were distilled over drying agent of calcium hydride under nitrogen prior to use. Polymerizations were carried out in Schlenk tubes by using a nitrogen flow to drive off the ethylene condensate for ADMET.

Characterization

^1H (500 MHz) and ^{13}C (125 MHz) NMR spectra were recorded on a Bruker DPX spectrometer using tetramethylsilane as an internal standard and $CDCl_3$ as a solvent. Melting point was determined by micro melting point apparatus (Yanoco). FTIR spectra were recorded on a Nicolet Nexus 670 in the region of 4000–400 cm^{-1} using KBr pellets. The HR-ESIMS was measured by a Bruker QTOF micromass spectrometer. UV-Vis absorption spectra were measured on a Cary 60 spectrometer. Gel permeation chromatography (GPC), equipped with a Waters 1515 Isocratic HPLC pump, a Waters 2414 refractive index detector, and a set of Waters Styragel columns (7.8 mm × 300 mm, 5 mm bead size; 10^3, 10^4, and 10^5 Å pore size), was used to measure the relative number- and weight-average molecular weights (M_n and M_w) and polydispersity index (PDI). The hydrodynamic diameter was determined by means of dynamic light scattering (DLS) analysis using a Malvern Zetasizer Nano-ZS light scattering apparatus (Malvern Instruments, UK) with a He-Ne laser (633 nm, 4 mW). The sample for transmission electron microscopy (TEM) testing was prepared by depositing a drop of the solution (1 mg/mL) on a carbon coated Cu grid, and TEM images were recorded on the JEOL2100F microscopes operating at 120 kV. Differential scanning calorimetry (DSC) was performed on a Netzsch 204F1 in nitrogen atmosphere. An indium standard was used for temperature and enthalpy calibrations. All the samples were heated from 50 °C to 250 °C and kept at 250 °C for 3 min to eliminate the thermal history. Then they were cooled to room temperature and heated again from 50 °C to 250 °C at a heating or cooling rate of 10 °C/min. Thermal gravimetric analysis (TGA) was performed using a SDTA851e/SF/1100 TGA Instrument under nitrogen flow at a heating rate of 10 °C/min from 50 °C to 800 °C. Cyclic voltammetry (CV) was carried out with an Autolab PGSTAT12 potentiostat from Eco Chemie coupled to an electrochemical cell with three electrodes. The scan rate is 100 mV/s. A glassy carbon electrode was used as the working electrode, a Pt wire as the counter, and Ag/AgCl was used as the reference electrode. Bu_4NPF_6 of CH_3CN solution (0.1 mol/L) was used as the supporting electrolyte, and Fc^+/Fc was used as the reference.

https://doi.org/10.1007/s10118-018-2067-1

Synthesis of *N,N'*-dodecanoic Acid 1,6,7,12-tetrachloroperylene-3,4,9,10-tetracarboxylic Bisimide Compound (1)

A mixture of 1,6,7,12-tetrachloroperylene-3,4,9,10-tetracarboxylic dianhydride (2.65 g, 5 mmol) and 12-aminododecanoic acid (2.58 g, 12 mmol) in propionic acid (40 mL) was heated to reflux at 140 °C for 36 h under a N_2 atmosphere. The resulting mixture was cooled and poured into water, filtrated, and washed with water until the filtrate reached neutrality. The crude solid was dried at 70 °C under vacuum. After being purified by column chromatography (silica gel) with a mixed solution (HAc/CH_2Cl_2 1/150 to 1/125, *V/V*) as an eluent, the orange-red powder compound **1** was obtained (4.02 g, yield 87%). ^{1}H-NMR ($CDCl_3$, δ, ppm): 8.69 (s, 4H, pery), 4.32–4.18 (m, 4H, $NC\underline{H}_2CH_2$), 2.45–2.31 (m, 4H, $CH_2C\underline{H}_2COOH$), 1.82–1.71 (m, 4H, $NCH_2C\underline{H}_2$), 1.70–1.62 (m, 4H, $C\underline{H}_2CH_2COOH$), 1.55–1.18 (m, 28H, $CH_2C\underline{H}_2CH_2$). ^{13}C-NMR ($CDCl_3$, δ, ppm): 178.78, 161.94, 134.75, 132.61, 130.81, 128.67, 123.29, 40.43, 33.42, 29.04, 28.68, 27.58, 26.48, 24.10.

Synthesis of PTCBI-functionalized α,ω-Diene Monomer (M1)

Compound **1** (2.12 g, 4 mmol) was firstly dispersed in 50 mL of anhydrous CH_2Cl_2. To this solution, 10-undecen-1-ol (2.58 g, 12 mmol), EDCI·HCl (0.92 g, 5.8 mmol) and DMAP (0.1 g, 0.8 mmol) were added under nitrogen atmosphere in ice-water bath and stirred for 2 h, then raised the reaction mixture to room temperature, and monitored the reaction by thin layer chromatography (TLC). After 5 days, the mixture was washed by dilute hydrochloric acid (5 × 30 mL) and water, and then dried with anhydrous $MgSO_4$. After filtration and removing the solvent, crude product was purified by column chromatography on silica gel using CH_2Cl_2/petroleum ether (1/1, *V/V*) as an eluent. The α,ω-diene monomer **M1** was obtained as red-orange powder (3.82 g, yield 95%). ^{1}H-NMR ($CDCl_3$, δ, ppm): 8.70 (s, 4H, pery), 5.87–5.76 (m, 2H, $CH_2{=}C\underline{H}CH_2$), 5.04–4.90 (m, 4H, $C\underline{H}_2{=}CHCH_2$), 4.28–4.18 (t, 4H, $COOC\underline{H}_2$), 4.10–4.01 (t, 4H, $NC\underline{H}_2CH_2$), 2.34–2.27 (t, 4H, $CH_2C\underline{H}_2COO$), 2.10–1.99 (m, 4H, $CH_2{=}CHC\underline{H}_2$), 1.80–1.24 (m, 64H, $C\underline{H}_2$ on alkyl chain). ^{13}C-NMR ($CDCl_3$, δ, ppm): 173.91, 161.90, 139.54, 135.46, 137.18, 131.16, 128.67, 128.59, 123.02, 114.11, 64.52, 40.98, 34.41, 33.78, 29.53, 29.49, 29.42, 29.34, 29.26, 29.24, 29.18, 29.10, 28.91, 28.65, 28.11, 27.06, 25.92, 25.02. IR (cm^{-1}): 3061, 2924, 2854, 1736, 1705, 1665, 1592, 1478, 1392, 1337, 1285, 1176, 1056, 992, 911, 845, 804, 751, 677, 605. HR-MS: Calcd. for $C_{70}H_{90}Cl_4N_2O_8Na$ $[M+Na]^+$: 1251.5332, Found: 1251.5336.

Representative Procedure for ADMET Polymerization (P1)

A 10 mL of Schlenk tube was charged with monomer **M1** (400 mg, 0.32 mmol) dissolved in 0.8 mL of toluene. In another 10 mL Schlenk tube, **Ru-II** (13 mg, 15 μmol) was dissolved in 0.2 mL of toluene. After degassed by three freeze-vacuum-thaw cycles, the catalyst solution of **Ru-II** was injected into the monomer solution with a syringe under vigorous stirring at 50 °C. The reaction was performed for 24–96 h followed by a slow purge of nitrogen to drive off the ethylene condensate. During the reaction time, a second aliquot of the mixture was withdrawn from the tube with a syringe and 1 mol% **Ru-II** was added at the predetermined time intervals to monitor the metathesis reaction by GPC. The resulting mixture gradually became viscous due to the increase of molecular weight, and the solvent of toluene partially evaporated. The polymerization was finally quenched by adding excess of ethyl vinyl ether with stirring for another 30 min. The mixture was poured into 20 mL of diethyl ether and the precipitate was isolated by filtration, dried under vacuum at 60 °C for 24 h to give the unsaturated polymer **P1** as an orange-red solid in moderate yields. ^{1}H-NMR ($CDCl_3$, δ, ppm): 8.70 (s, 4H, pery), 8.70 (s, pery), 5.28 (s, $C\underline{H}{=}C\underline{H}$ on backbone), 4.26–4.18 (t, $COOC\underline{H}_2$), 4.10–4.01 (t, $NC\underline{H}_2CH_2$), 2.36–2.17 (t, $CH_2C\underline{H}_2COO$), 2.14–1.96 (m, $CH{=}CHC\underline{H}_2$), 1.82–1.22 (m, $C\underline{H}_2$ on alkyl chain). ^{13}C-NMR ($CDCl_3$, δ, ppm): 173.98, 161.83, 137.22, 135.42, 131.17, 130.28, 129.68, 128.65, 128.60, 123.00, 64.54, 40.95, 34.43, 33.76, 29.53, 29.48, 29.43, 29.36, 29.24, 29.27, 29.20, 29.13, 28.94, 28.62, 28.10, 27.04, 25.95, 25.06. IR (cm^{-1}): 3061, 2924, 2854, 1728, 1705, 1638, 1592, 1470, 1384, 1332, 1265, 1176, 1056, 968, 911, 845, 804, 762, 680, 605.

General Procedure for Hydrogenation of Unsaturated Polymer (HP1)

Typically, **P1** (250 mg), TSH (270 mg, 1.45 mmol), and BHT (50 mg) were weighed and added into a 100 mL Schlenk flask. Then, 15 mL of toluene was added to obtain a dark-red suspension. The flask was connected to a reflux condenser equipped with a bubbling tube and placed in an oil bath at 120 °C under vigorous stirring. After 6 h, the reaction was stopped on cooling to room temperature, and another equal supply of TSH was added. The reaction was allowed for another 6 h at 130 °C. The mixture was poured into ethyl ether, and the precipitated solid was redissolved in 1 mL of CH_2Cl_2 to give a viscous solution that was added dropwise into 20 mL of cold methanol to obtain a red precipitate. After filtration and vacuum dryness, the saturated polymer **HP1** was obtained in 95% yield. ^{1}H-NMR ($CDCl_3$, δ, ppm): 8.70 (s, pery), 4.23–4.18 (t, $COOC\underline{H}_2$), 4.10–4.03 (t, $NC\underline{H}_2CH_2$), 2.37–2.07 (t, $CH_2C\underline{H}_2COO$), 2.11–1.94 (m, $CH{=}CHC\underline{H}_2$), 1.85–1.20 (m, $C\underline{H}_2$ on alkyl chain). ^{13}C-NMR ($CDCl_3$, δ, ppm): 173.78, 161.73, 137.21, 135.42, 131.23, 128.81, 128.57, 123.02, 64.59, 40.98, 34.41, 33.56, 29.63, 29.51, 29.41, 29.26, 29.14, 29.28, 29.22, 29.15, 28.98, 28.65, 28.15, 27.01, 25.90, 25.05. IR (cm^{-1}): 3061, 2925, 2854, 1728, 1705, 1638, 1597, 1475, 1384, 1330, 1265, 1173, 1056, 911, 845, 804, 762, 680, 605.

RESULTS AND DISCUSSION

Synthesis of Functional Diene Monomer

The PTCBI-functionalized α,ω-diene monomer **M1** was synthesized according to the procedures reported in the literature[14]. The chemical structure and synthetic route of

https://doi.org/10.1007/s10118-018-2067-1

M1 are shown in Scheme 1. Firstly, the imidization reaction of TCPTCDA with 12-aminododecanoic acid was carried out, giving the symmetrical compound **1** with two reactive carbonyl groups. Then **M1** with aromatic PTCBI and aliphatic alkyl spacer between diene end groups was easily obtained by subsequent esterification reaction of **1** with 10-undecen-1-ol in CH_2Cl_2 solution at room temperature. The crude product was purified by column chromatography on silica gel using CH_2Cl_2/petroleum ether (1/2–1/1 *V*/*V*) as an eluent to give **M1** as a red-orange powder.

NMR and HR-MS spectroscopies were employed to confirm the chemical structures. Fig. 1(A) shows the ^{1}H-NMR spectrum of monomer **M1**. The proton signal at 8.70 ppm is assigned to the aromatic proton on PTCBI branch. The terminal double protons appear at 5.87–5.76 and 5.04–4.90 ppm, and the integration values of peaks at 8.70, 5.87–5.76, and 5.04–4.90 ppm are nearly 2:1:2, indicating that the PTCBI core is successfully attached to 10-undecen-1-ol. ^{13}C-NMR measurement was also employed to characterize the structure of **M1** (Fig. 1D). The strong resonances of C=O in ester and imide groups from **M1** are observed at about 173.91 and 161.90 ppm (Fig. S1 in electronic supplementary information, ESI), respectively. The resonance signals of carbons at 135.46, 137.18, 131.16, 128.67, 128.59, and 123.02 ppm, are attributable to the chemical structure of perylene core. The other two peaks at 139.54 and 114.11 ppm are assigned to the unsaturated carbon on terminal double bond. The IR spectrum of **M1** (Fig. 2) shows the characteristic stretching of PTCBI branch, which are present at 1705 and 1665 cm^{-1}. The shoulder peaks at 2924 and 2854 cm^{-1} (not shown here) are assigned to the saturated CH_2 group, and the characteristic absorption bands at 1392, 1285, 1056, and 677 cm^{-1} are attributed to the stretching vibration of C—N, C=O, C—O—C, and the out-of-plane bending vibrations of C = C — H group, respectively. Besides, the vibration of terminal CH=CH_2 group at 992 cm^{-1} is also observed. Furthermore, the molecular weight of **M1** by HR-MS analysis is in good accordance with the calculated value. All of the above results assure that **M1** has been successfully synthesized.

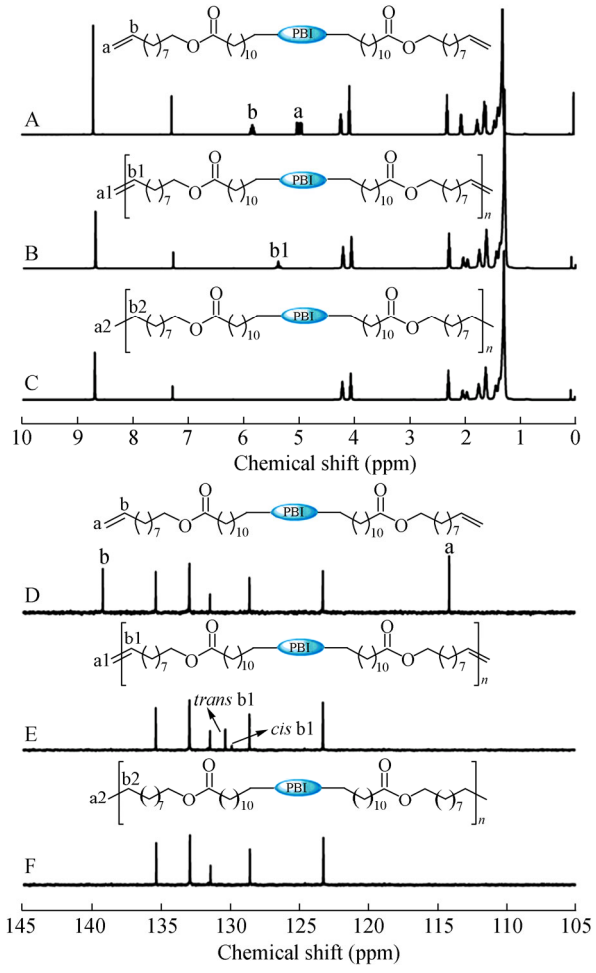

Fig. 1 (A–C) ^{1}H-NMR and (D–F) ^{13}C-NMR spectra of α,ω-diene monomer, ADMET polymer, and hydrogenated polymer

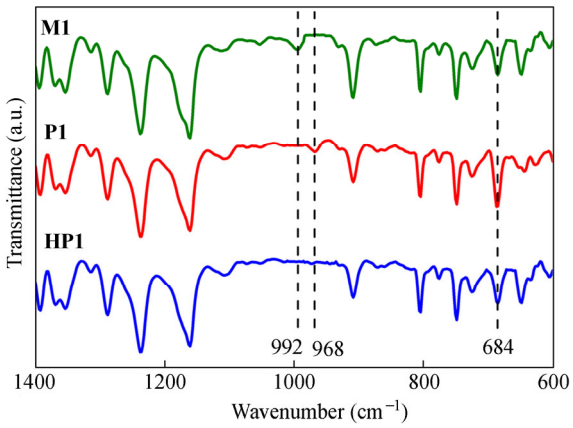

Fig. 2 FTIR spectra of α,ω-diene monomer **M1**, ADMET polymer **P1**, and hydrogenated polymer **HP1**

ADMET Polymerization and Hydrogenation

The ADMET polymerization of **M1** was carried out in chloroform and toluene at 60 °C for 24–96 h using **Ru-II** as a catalyst due to its high catalytic performance. During the polymerization, an aliquot of the reactive mixture was withdrawn from the tube by a syringe and another 1 mol% **Ru-II** was added at the predetermined 24 h intervals to monitor the metathesis reaction by GPC. After purification, the unsaturated polymer **P1** was obtained as a dark-red solid. Subsequently, exhaustive hydrogenation of **P1** afforded saturated PE with PTCBI defects on every 44th carbon. Our previous report on the synthesis of saturated hybrid polymer illustrated that the hydrogenation degree of double bonds by TSH in 4 h was relatively high; however, a few unsaturated double bonds still remained[15]. In order to ensure complete hydrogenation, two batch feedings of TSH were used at a time interval of 6 h. After hydrogenation, the polymer was precipitated in petroleum ether, resulting in orange saturated periodic polymer **HP1**.

The structures of representative polymers were characterized by NMR spectroscopy. As compared with **M1**, the proton signals at 5.80–5.65 and 4.95–4.75 ppm (Fig. 1B) and the carbon signals at 139.54 and 114.11 ppm (Fig. 1E), assigned to the terminal alkenes (a, b) disappeared after

https://doi.org/10.1007/s10118-018-2067-1

ADMET polymerization, while the protons of newly formed internal alkenes (b1) on the polymer main chain appeared at 5.28 ppm (Fig. 1B). Also, the carbon signals at 130.28 and 129.68 ppm (Fig. 1E) were attributed to the internal *trans* and *cis* double bonds[16, 17]. After exhaustive hydrogenation, the signals of internal alkenyl protons in **P1** disappeared completely in NMR spectra (Figs. 1C and 1F), indicating the complete hydrogenation by using the above-mentioned protocol. In particular, hydrolysis of the ester groups that might be caused by the generated *p*-toluenesulfonic acid did not occur because the aromatic proton (8.60 ppm) in **HP1** still remained. Moreover, IR spectroscopy further confirmed the structures of as-obtained polymers. When comparing the IR spectra of **P1** and **HP1** with that of **M1** (Fig. 2), we observed clearly that the absorption bands exhibited no significant change except the disappearance of terminal double bonds (992 cm^{-1}). Meanwhile, a new absorption peak appeared at 968 cm^{-1}, and the peak at 684 cm^{-1} strengthened, which were ascribed to the *trans* and *cis* double bonds on the polymer backbone, respectively. This result is consistent with the ^{13}C-NMR results of the *trans* and *cis* double bonds for **P1**. As for saturated **HP1**, however, the *trans* double bonds at 968 cm^{-1} disappeared and the *cis* double bonds at 684 cm^{-1} weakened obviously. Based on these results, we can conclude that the obtained unsaturated **P1** is completely converted to the saturated **HP1**.

As an initial attempt, ADMET reaction of **M1** was carried out in $CHCl_3$, the orange-red color gradually changed to red, and finally dark-red solid **P1** was obtained in a high yield by precipitating the reaction mixture from excess ethyl ether. The polymerization conditions and results are listed in Table 1.

Table 1 Conditions for the ADMET polymerization of monomers [a] and analytical data of the resulting polymers

Polymer	*t* (h)	Yield [b] (%)	M_n [c] (kDa)	PDI [c]	T_d [d] (°C)	T_g [e] (°C)
P1a'	24	80.4	18.2	2.04	–	–
P1b'	48	87.5	24.7	1.92	–	–
P1c'	72	95.5	30.4	1.85	298	46
P1d'	96	98.7	80.1	1.65	–	–
HP1c'	–	–	30.1	1.64	320	34
P1a	24	60.4	16.3	2.12	–	–
P1b	48	67.1	24.6	1.85	–	–
P1c	72	73.2	30.1	1.67	–	–
P1d	96	74.3	30.8	1.54	312	63
HP1d	–	–	30.7	1.52	341	47

[a] Reaction conditions: $[Monomer]_0$:$[Catalyst]_0$ = 50:1, $[Monomer]_0$ = 0.5 mol/L, temperature = 60 °C, polymerizations were conducted in chloroform (**P1a'**–**P1d'**) or toluene (**P1a**–**P1d**) with **Ru-II** as the catalyst; [b] Obtained gravimetrically after purification from the dried polymer; [c] Number-average molecular weight (M_n) and polydispersity index (PDI) determined by GPC in THF relative to monodispersed polystyrene standards; [d] Decomposition temperature at 5% weight loss determined by TGA; [e] Glass transition temperature determined by DSC

GPC traces of **P1** obtained in chloroform at different reaction time are shown in Fig. 3(a). With the progress of polymerization, the elution curves gradually shifted to higher molecular weight region (from 18.2 kDa to 80.1 kDa) and PDI became narrower (ranging from 2.04 to 1.65), indicating

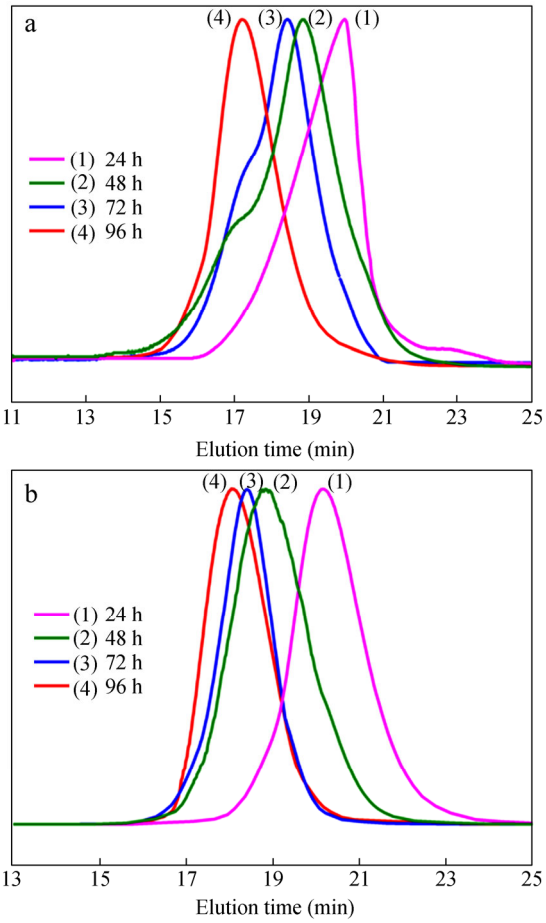

Fig. 3 GPC traces of polymer prepared *via* ADMET polymerization in (a) $CHCl_3$ and (b) toluene

the increase of repeated monomeric unit number. It is in good agreement with the feature of step-growth polymerization. Nevertheless, when the polymerization of ADMET was conducted in toluene, a very different result was obtained. The isolated **P1** had distinct reduced molecular weight from 16.3 kDa to 30.8 kDa with PDI ranging from 2.12 to 1.54 (Table 1 and Fig. 3b), and the yield even decreased to about 60%. We deduced that such a phenomenon was possibly due to the *in situ* self-assembly of **P1** during polymerization in toluene, leading to the active species imbedded ultimately. Consequently, the molecular weight of **P1** increased slowly even prolonged reaction time to 96 h (Fig. 3b). In addition, two types of saturated periodic **HP1**s had the similar molecular weights, and were close to their precursors because we selected **P1**s with the proximate molecular weights as the starting materials. This also sufficiently attested no degradation under the used hydrogenation conditions.

Self-assembled Morphology

As discussed above, the self-assembly of **P1** might occur in toluene, thus, the structure of **P1** was analyzed by DLS and TEM measurements. Figure 4(a) exhibits the size of **P1** with the average hydrodynamic diameter of 300 nm in toluene. The morphology of **P1** was examined by TEM. The sample was prepared by dropping the dilute solution of crude reaction

https://doi.org/10.1007/s10118-018-2067-1

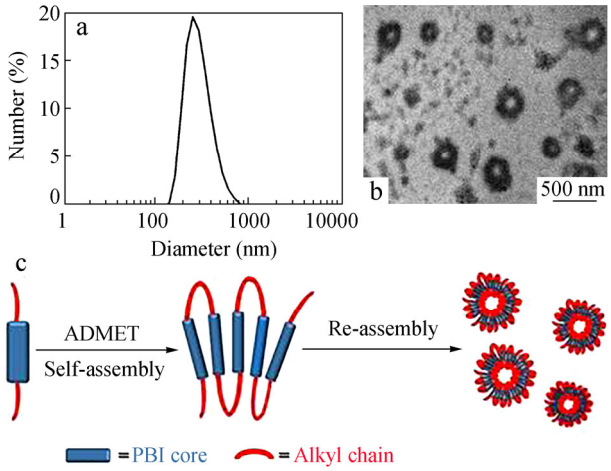

Fig. 4 The self-assembly of **P1**: (a) size determined by means of DLS in toluene, (b) TEM image, and (c) the schematic of hollow curvature-shaped architecture formation

liquid onto mica. Interestingly, the TEM image in Fig. 4(b) shows a hollowed circle structure in comparatively uniform with diameter ranging from 175–250 nm, smaller than that obtained from DLS analysis due to the solvation of polymer in solution. The self-assembly of **P1** was possibly driven by π-π stacking interactions between the adjacent perylene cores along one-dimensional long axis, and stabilized by surrounding long alkyl chains as illustrated in Fig. 4(c).

We speculate that when ADMET polymerized in toluene, **P1** spontaneously self-assembled into stable fan-like architecture with high degree of curvature, driven by the π-π stacking interaction between perylene bisimide cores, the stereo-hindrance effect, the solvent effect, as well as the folding ability of flexible alkyl chain. Then, some of curvature-shaped architecture spontaneously released the strain and surface energy, leading to the formation of hollow curvature-shaped architecture, which could further enhance the π-π interaction between PTCBI moieties. However, many smaller agglomerates without hollow space were also observed in addition to the hollow cylindrical structure, which was possibly caused by the crystallization of residual **M1** or isolated curvature-shaped architecture. For **P1'** obtained in $CHCl_3$, it has an average diameter of 9 nm without any unique architecture (Figs. S4 and S5, in ESI), suggesting that solvent is the most important promoter for the self-assembly of PTCBI in-chain PE in the reaction system. In short, both of these analyses strongly indicate that the PTCBI in-chain PE can spontaneously self-assemble into stable hollow circles during ADMET polymerization in toluene. Such a process is convenient because there is no need for post-treating, adjusting the composition, and tailing the solubility of block copolymers.

Spectroscopic and Redox Properties

The PTCBI-functionalized monomer **M1** and unsaturated **P1** were readily soluble in various organic solvents. The electronic and photophysical properties of the monomer and polymer were investigated at room temperature by UV-Vis absorption and emission spectroscopy in $CHCl_3$ solution. As shown in Fig. 5(a), the characteristic absorption of **P1** is analogous to that of **M1**, suggesting that the non-conjugated polymer backbone derived from ADMET polymerization had no effect on the spectral properties. The maximum absorption of ADMET polymer at 518 nm (λ_{max}) with a strongly pronounced vibronic fine structure is observed in $CHCl_3$ solution. It belongs to the electronic S_0-S_1 transition with a transition dipole moment along molecular axis[18], and a second absorption band emerged at lower wavelengths (400–460 nm), which is attributed to the electronic S_0-S_2 with a transition dipole moment perpendicular to the long molecular axis[19].

Besides, **P1** displayed solvatochromic behavior (Fig. 5b), and the values of λ_{max} changed in different solvents with the following order: 514 nm (THF) < 517 nm (CH_2Cl_2, $CHCl_3$) < 528 nm (toluene). The typical fluorescence changes are shown in Fig. 5(c). Emission spectrum was measured under illumination in $CHCl_3$ solution with the excited wavelength at 522 nm, and Φ_f was estimated using 9,10-diphenyl-anthracene (Φ = 90%) as a standard. The results show that the photoluminescence quantum yield was 64% for **M1** at room temperature under ambient atmosphere, and decreased to 45% after polymerization (Fig. 5c). It may demonstrate that the π-π stacking of **P1** was enhanced. In order to get an insight into the intrinsic electrochemical properties of PTCBI functionalized **P1**, the CV analysis was performed with a film (on glassy carbon electrode). The film exhibited reversible oxidative and reductive properties, and displayed two successive reversible mono-electronic reduction waves around –0.96 and –0.78 V, respectively (Fig. 5d). According to the literature report[18], the low-lying lowest unoccupied molecular orbital (LUMO) energy could be obtained from the onset reduction potential (E_{red}^{onset}) by the Eq. (1):

$$E_{LUMO} = -4.4 + E_{red}^{onset} \quad (1)$$

The LUMO energy of **P1** is calculated to be –3.62 eV, which is in accordance with structurally defined high-LUMO-level 66π-[70] fullerene derivatives[20], suggesting that this type of PTCBI derivatives could be used in solar cell devices with higher open-circuit voltage.

Thermal Properties

Thermal properties of polymers were systematically investigated by TGA and DSC. The thermal decomposition temperatures (T_d) at 5% weight loss of **P1d**, **P1c'**, **HP1d**, and **HP1c'** were 312, 298, 341, and 320 °C (Table 1, Figs. 6a and S6) respectively. These results are similar to those of previously reported PE with one single ethyl acrylate on every periodic number of carbons and PTCBI branched PE[21], indicating the high thermal stability. Besides, the unsaturated **P1c'** and **P1d** almost decomposed completely at 800 °C, while about 32% and 22% of weights were still retained for the saturated **HP1c'** and **HP1d**, indicating an obviously higher residue than that of the hydrogenated ethylene-ethyl acrylate polymers[21], and the excellent thermal stability of PTCBI-contained PE.

https://doi.org/10.1007/s10118-018-2067-1

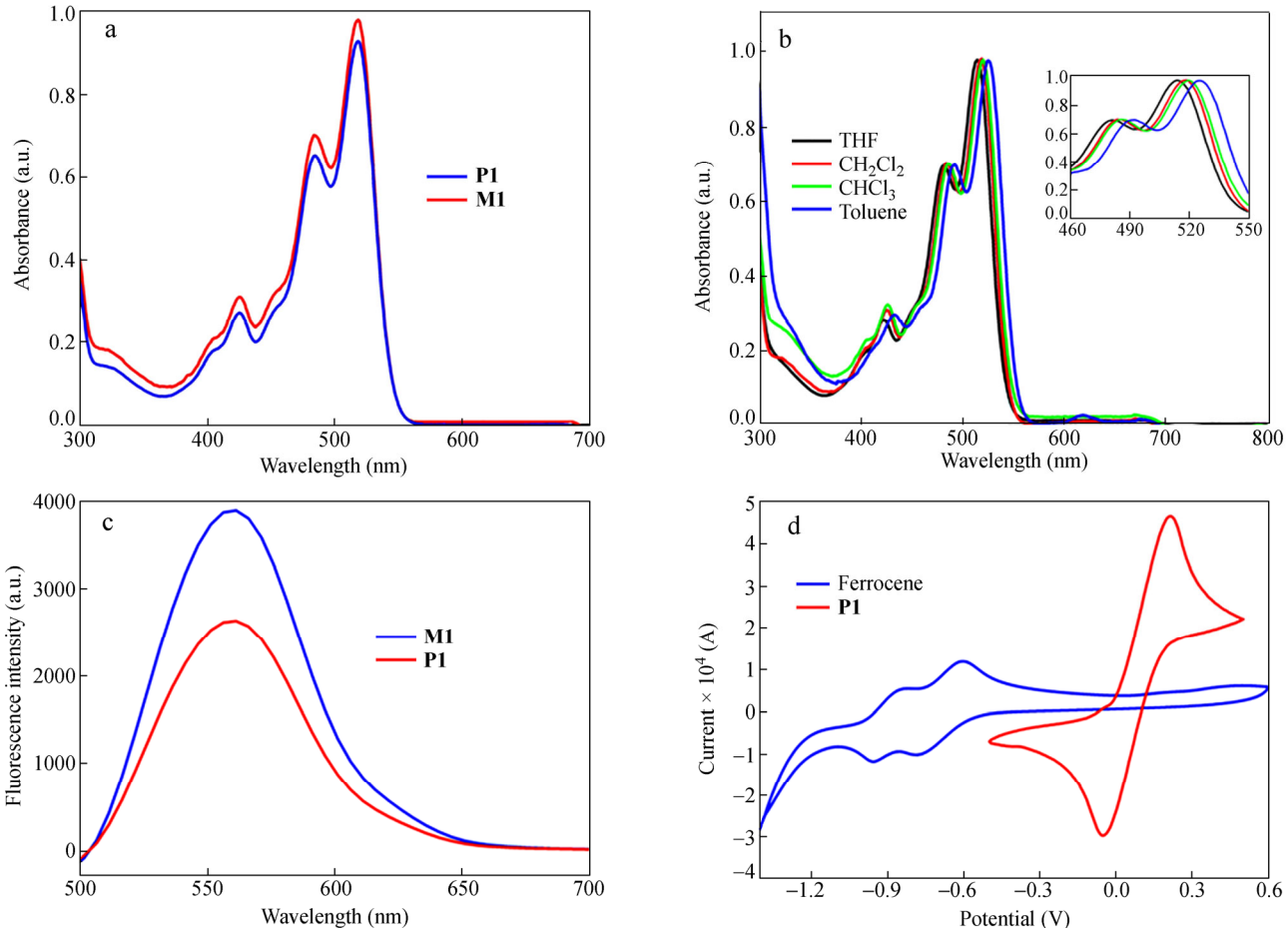

Fig. 5 (a, b) UV-Vis spectra, (c) emission spectra, and (d) CV curves of ADMET polymer

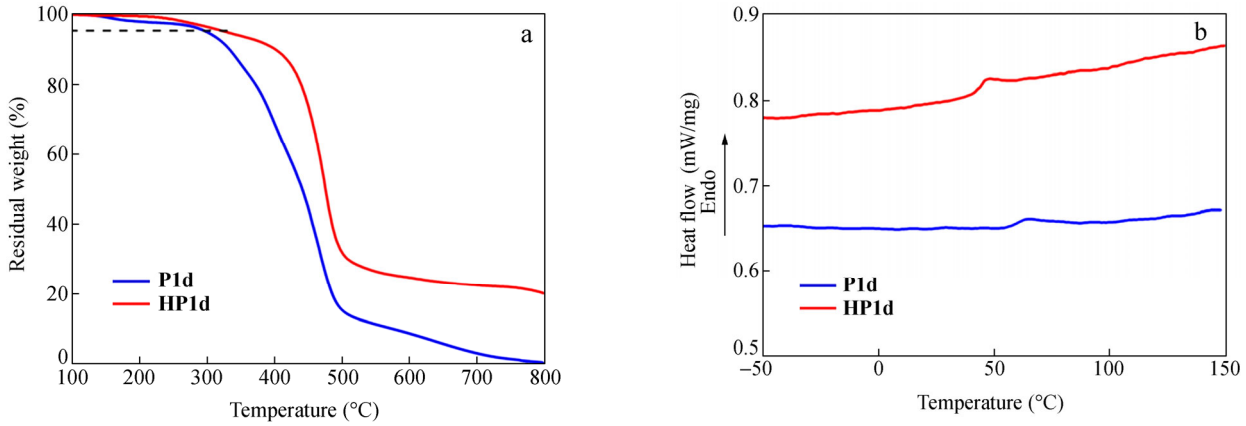

Fig. 6 Thermal properties of **P1d** and **HP1d**: (a) TGA traces; (b) DSC curves

The DSC profiles for **P1** and **HP1** show an obvious correlation between PTCBI moiety and thermal behavior. As depicted in Fig. 6(b), precise incorporation of PTCBI moiety between every 42nd methylene units on polymer backbone generated polyolefin with higher T_g of 63 °C (**P1d**) and PE with relatively lower T_g of 47 °C (**HP1d**), respectively. Additionally, the values of T_g reduced to 46 and 34 °C for **P1c'** and **HP1c'** (Fig. S7, in ESI), indicating that the segment motion was much easier than that of **P1d** and **HP1d**. This result is expected, because the bulky PTCBI moieties distributed precisely in the polyolefin backbone and formed an ordered structure in toluene, which further inhibited the flexible movement of polymer chain. The T_g of PTCBI in-chain polyolefin shifted to much higher temperature relative to perfect precision phenylboronic acid in-chain polyolefins (from –28 °C to –4 °C)[22] and is close to that of PTCBI out-chain analogue (51–76 °C)[23]. That means the strong π-π stacking interaction of PTCBI moieties may be responsible for the restricted segment motion. Different from PE-PERY copolymers[24], the DSC thermograms for these

https://doi.org/10.1007/s10118-018-2067-1

polymers showed no melting transition up to 200 °C. PE is a typical (semi)crystalline polymer[15], while the inherently crystalline behavior was disturbed by the ordered structure, even though the length of methylene groups between PTCBI moieties was more than 20. Thereby, longer methylene spacer and weaker interaction of in-chain moieties may reduce this type of disturbance. Combined with previous results[23], it can be deduced that regardless of PTCBI moieties located in PE main-chain or side-chain, the inherent crystallization ability is totally lost.

CONCLUSIONS

In summary, we have demonstrated a facile synthetic pathway to produce a precision PTCBI-sequenced PEs *via* ADMET polymerization and subsequent hydrogenation protocol. Such polymer is of particular interest for the optoelectronic applications since it not only has a precise sequence distribution of in-chain moieties on every 42nd methylene units, but also possesses a potentially useful building block of PTCBI and a rigid aryl chromophore capable of electron transport as the *n*-type semiconductor. The precision PTCBI in-chain PE showed good thermal stability with relatively higher T_g (47 °C) and T_d (321–341 °C). Also, the polymer displayed light absorption in a wider wavelength range (200–575 nm) and higher LUMO energy level (–3.62 eV), which could endow the solar cell devices with high open-circuit voltage. Although it exhibited no crystallinity of PE likely due to the overlapping of PTCBI defects, the polymer *in situ* self-assembled into the regular hollow cylinders. This feature can enhance π-π interaction between PTCBI defects, which is interesting for the prospective application in solar cells and other optoelectronic devices. Further studies will be focused on investigating the influence of PTCBI location (in or out-chain) and topology on the functionality, especially on the electron mobility, directing to utilize these new polymers as functional materials for optoelectronic application.

Electronic Supplementary Information

Electronic supplementary information (ESI) is available free of charge in the online version of this article at http://dx.doi.org/10.1007/s10118-018-2067-1.

ACKNOWLEDGMENTS

This work was financially supported by the National Natural Science Foundation of China (No. 21774107), the Jiangsu Government Scholarship for Overseas Studies, and the Initial Scientific Research Foundation of Yancheng Institute of Technology (No. KJC2014002).

REFERENCES

1 Zhao, X. G.; Ma, L. C.; Zhang, L.; Wen, Y. G.; Chen, J. M.; Shuai, Z. G.; Liu, Y. Q.; Zhan, X. W. An acetylene-containing perylene diimide copolymer for high mobility *n*-channel transistor in air. Macromolecules 2013, 46(6), 2152–2158.
2 Rajaram, S.; Shivanna, R.; Kandappa, S. K.; Narayan, K. S. Nonplanar perylene diimides as potential alternatives to fullerenes in organic solar cells. J. Phys. Chem. Lett. 2012, 3(17), 2405–2408.
3 Lindner, S. M.; Hüttner, S.; Chiche, A.; Thelakkat, M.; Krausch, G. Charge separation at self-assembled nanostructured bulk interface in block copolymers. Angew. Chem. Int. Ed. 2006, 45(20), 3364–3368.
4 Rajaram, S.; Armstrong, P. B.; Kim, B. J.; Fréchet, J. M. Effect of addition of a diblock copolymer on blend morphology and performance of poly(3-hexylthiophene): perylene diimide solar cells. Chem. Mater. 2009, 21(9), 1775–1777.
5 Zhang, Q.; Cirpan, A.; Russell, T. P.; Emrick, T. Donor-acceptor poly(thiophene-block-perylene diimide) copolymers: synthesis and solar cell fabrication. Macromolecules 2009, 42(4), 1079–1082.
6 Huang, J.; Wu, Y.; Fu, H.; Zhan, X.; Yao, J.; Barlow, S.; Marder, S. R. Photoinduced intramolecular electron transfer in conjugated perylene bisimide-dithienothiophene systems: a comparative study of a small molecule and a polymer. J. Phys. Chem. A 2009, 113(17), 5039–5046.
7 Jiang, W.; Xiao, C.; Hao, L.; Wang, Z.; Ceymann, H.; Lambert, C.; Motta, S. D.; Negri, F. Localization/delocalization of charges in bay-linked perylene bisimides. Chem. Eur. J. 2012, 18(22), 6764–6775.
8 Singh, R.; Giussani, E.; Mróz, M. M.; Fonzo, F. D.; Fazzi, D.; González, J. C.; Oldridge, L.; Vaenas, N.; Kontos, A. G.; Falaras, P.; Grimsdale, A. C.; Jacob, J.; Mullen, K.; Keivanidis, P. E. On the role of aggregation effects in the performance of perylene- diimide based solar cells. Org. Electron. 2014, 15(7), 1347–1361.
9 Song, S. F.; Guo, Y. T.; Wang, R. Y.; Fu, Z. S.; Xu, J. T.; Fan, Z. Q. Synthesis and crystallization behavior of equisequential ADMET polyethylene containing arylene ether defects: remarkable effects of substitution position and arylene size. Macromolecules 2016, 49(16), 6001–6011.
10 Lv, A.; Cui, Y.; Du, F. S.; Li, Z. C. Thermally degradable polyesters with tunable degradation temperatures *via* postpolymerization modification and intramolecular cyclization. Macromolecules 2016, 49(22), 8449–8458.
11 Zhang, H.; Liu, F.; Cao, J.; Ling, L.; Sun, R. F. Ferrocene-containing polymers synthesized by acyclic diene metathesis (ADMET) polymerization. Chinese. J. Polym. Sci. 2016, 34(2), 242–252.
12 Ding, L.; Song, W.; Jiang, R. Y.; Zhu, L. A straightforward approach for one-pot synthesis of noncovalently connected graft copolymers with unique self-assembly nanostructures. Polym. Chem. 2016, 7(45), 6992–7001.
13 Li, Q. B.; Wang, T. S.; Ma, C.; Bai, W.; Bai, R. K. Facile and highly efficient strategy for synthesis of functional polyesters *via* tetramethyl guanidine promoted polyesterification at room temperature. ACS Macro Lett. 2014, 3(11), 1161–1164.
14 Song, W.; Han, H. J.; Wu, J. H.; Xie, M. R. Ladder-like polyacetylene with excellent optoelectronic properties and regular architecture. Chem. Commun. 2014, 50(85), 12899–12902.
15 Xie, M. R.; Han, H. J.; Jin, O. Y.; Du, C. X. Synthesis of ionic hybrid polymers with polyhedral oligomeric silsesquioxane pendant by acyclic diene metathesis polymerization and characterization. Acta Chim. Sinica 2013, 71(10), 1441–1445.
16 Thompson, D.; Yamakado, R.; Wagener, K. B. Extending the methylene spacer length of ADMET hydroxy-functionalized polymers. Macromol. Chem. Phys. 2014, 215(12), 1212–1217.
17 Rojas, G. Wagener, K. B. Precisely and irregularly sequenced ethylene/1-hexene copolymers: a synthesis and thermal study. Macromolecules 2009, 42(6), 1934–1947.

18 Li, Y. F.; Cao, Y.; Gao, J.; Wang, D.; Yu, G.; Heeger, A. J. Electrochemical properties of luminescent polymers and polymer light-emitting electrochemical cells. Synth. Met. 1999, 99(3), 243–248.
19 Gvishi, R.; Reisfeld, R.; Burshtein, Z. Spectroscopy and laser action of the "red perylimide dye" in various solvents. Chem. Phys. Lett. 1993, 213(3-4), 338–344.
20 Xiao, Z.; Matsuo, Y.; Soga, I.; Nakamura, E. Structurally defined high-LUMO-level 66π-[70]fullerene derivatives: synthesis and application in organic photovoltaic cells. Chem. Mater. 2012, 24(13), 2572–2582.
21 Baughman, T. W.; Sworen, J. C.; Wagener, K. B. Sequenced ethylene-propylene copolymers: effects of short ethylene run lengths. Macromolecules 2006, 39(15), 5028–5036.
22 Simocko, C.; Young, T. C.; Wagener, K. B. ADMET polymers containing precisely spaced pendant boronic acids and esters. Macromolecules 2015, 48(16), 5470–5473.
23 Song, W.; Wu, J. H.; Yang, G. D.; Han, H. J.; Xie, M. R.; Liao, X. J. Precise perylene bisimide-substituted polyethylene with high glass transition temperature and ordered architecture. RSC Adv. 2015, 5(84), 68765–68772.
24 Nielsen, C. B.; Veldman, D.; Rapun, R. M.; Janssen, R. A. J. Copolymers of polyethylene and perylenediimides through ring-opening metathesis polymerization. Macromolecules 2008, 41(4), 1094–1103.

https://doi.org/10.1007/s10118-018-2067-1